Natural Resources Canada | Ressources naturelles Canada

GEOLOGICAL SURVEY OF CANADA
OPEN FILE 8205

Thermokarst ponding, North Slave region, Northwest Territories

P.D. Morse, T.L. McWade, and S.A. Wolfe

2017

GEOLOGICAL SURVEY OF CANADA
OPEN FILE 8205

Thermokarst ponding, North Slave region, Northwest Territories

P.D. Morse[1], T.L. McWade[2], and S.A. Wolfe[1]

[1]Geological Survey of Canada, 601 Booth Street, Ottawa, Ontario
[2]Carleton University, 1125 Colonel By Drive, Ottawa, Ontario

2017

doi:10.4095/300531

This publication is available for free download through GEOSCAN (http://geoscan.nrcan.gc.ca/).

Recommended citation
Morse, P.D., McWade, T.L., and Wolfe, S.A., 2017. Thermokarst ponding, North Slave region, Northwest Territories; Geological Survey of Canada, Open File 8205, 1 .zip file. doi:10.4095/300531

Publications in this series have not been edited; they are released as submitted by the author.

ABSTRACT

This open file provides an inventory of thermokarst pond development between 1945 and 2005 in a study area that is representative of the southern North Slave region between Behchoko and Yellowknife, Northwest Territories. The primary purpose of this inventory is to approximate the location and size of thermokarst ponds in a study area representative of the region to assist in better understanding present and future permafrost conditions. Because construction of the GNWT Highway 3 in the mid-1960s utilized locally-available fine-grained materials sourced along the right-of-way, we examine potential thermokarst initiation at those sites and compare ponding adjacent to the highway with results for the region. The inventory and database were prepared to evaluate the dominant controls on the distribution of thermokarst in the region, and the potential influence that highway construction may have had on thermokarst development. The accompanying shapefile format data can be used in a GIS to place areas of thermokarst ponds onto digital maps for referencing.

DISCLAIMER

Her Majesty the Queen in right of Canada, as represented by the Minister of Natural Resources ("Canada"), does not warrant or guarantee the accuracy or completeness of the information ("Data") and does not assume any responsibility or liability with respect to any damage or loss arising from the use or interpretation of the Data.

The Data are intended to convey regional trends and should be used as a guide only. The Data should not be used for design or construction at any specific location, nor are the Data to be used as a replacement for the types of site-specific geotechnical investigations.

TABLE OF CONTENTS

Page

LIST OF FIGURES

Page

LIST OF TABLES

Page

1 INTRODUCTION

In the North, permafrost terrain is a foundation for infrastructure. It provides the environmental settings for a diverse array of flora and fauna relied upon by northern society, and the distribution of permafrost terrain affects interactions between surface and groundwater resources. Thus it is significant that permafrost degradation has been observed in many northern locations, and these changes are expected to have broad reaching effects on the North and its people. Therefore, characterization and quantification of permafrost change is essential for the development of effective adaptation measures and strategies.

Permafrost degradation occurs naturally due to warming climate or by changes to local surface conditions such as forest fire (*e.g.,* Zhang *et al.* 2015). Numerous examples of permafrost degradation initiated by human activity that disturbed the ground thermal regime (French 2007). Thermokarst is the process by which degradation of ice-rich permafrost creates characteristic landforms. Thermokarst terrain develops with ground settlement following melting of ground ice, and it is often indicated by water ponding in the resultant depressions. Surface water mapping is becoming an increasingly important tool to characterize thermokarst dynamics (*e.g.,* Olthof *et al.* 2015).

For much of Northern Canada, little detailed information about thermokarst exists. For example, in the North Slave region, NWT (Figure 1a), lake-level recession during the Holocene has giving rise to discontinuous permafrost (Heginbottom *et al.* 1995; Morse *et al.* 2015). Permafrost likely aggraded into these sediments in a time-transgressive manner with terrestrial emergence (Wolfe and Morse 2016). The fine-grained sediments are commonly ice rich to depths exceeding 8 m (Wolfe *et al.* 2011a, 2014b, 2015). Permafrost in this region is in thermal disequilibrium and is warming (Morse *et al.* 2015; Wolfe *et al.* 2015), and modelling suggests permafrost extent will continue to decline (Zhang *et al.* 2014). Differential subsidence of infrastructure has been observed in the city of Yellowknife (Wolfe *et al.* 2014a) and along sections of Northwest Territories Highway 3, which connects the city year-round with the south (BGC 2011; Seto *et al.* 2012; Stevens *et al.* 2012b). Subsidence typically accompanies thermokarst and occurs in this region (Figure 1b), but the distribution and activity of thermokarsthas not been assessed.

This report presents data regarding the changing condition of thermokarst ponds in the southern North Slave region. Thermokarst development (new ponding) in the North Slave region is detected by comparing historic and modern remotely sensed data sets available from 1945, 1961, and 2005. The primary purpose of this inventory is to approximate the location and size of thermokarst ponds in a study area representative of the region to assist in better understanding present and future permafrost conditions. As permafrost and ground ice are associated with the distribution of fine-grained deposits, we hypothesis that thermokarst may be more widespread at lower elevations where such deposits are

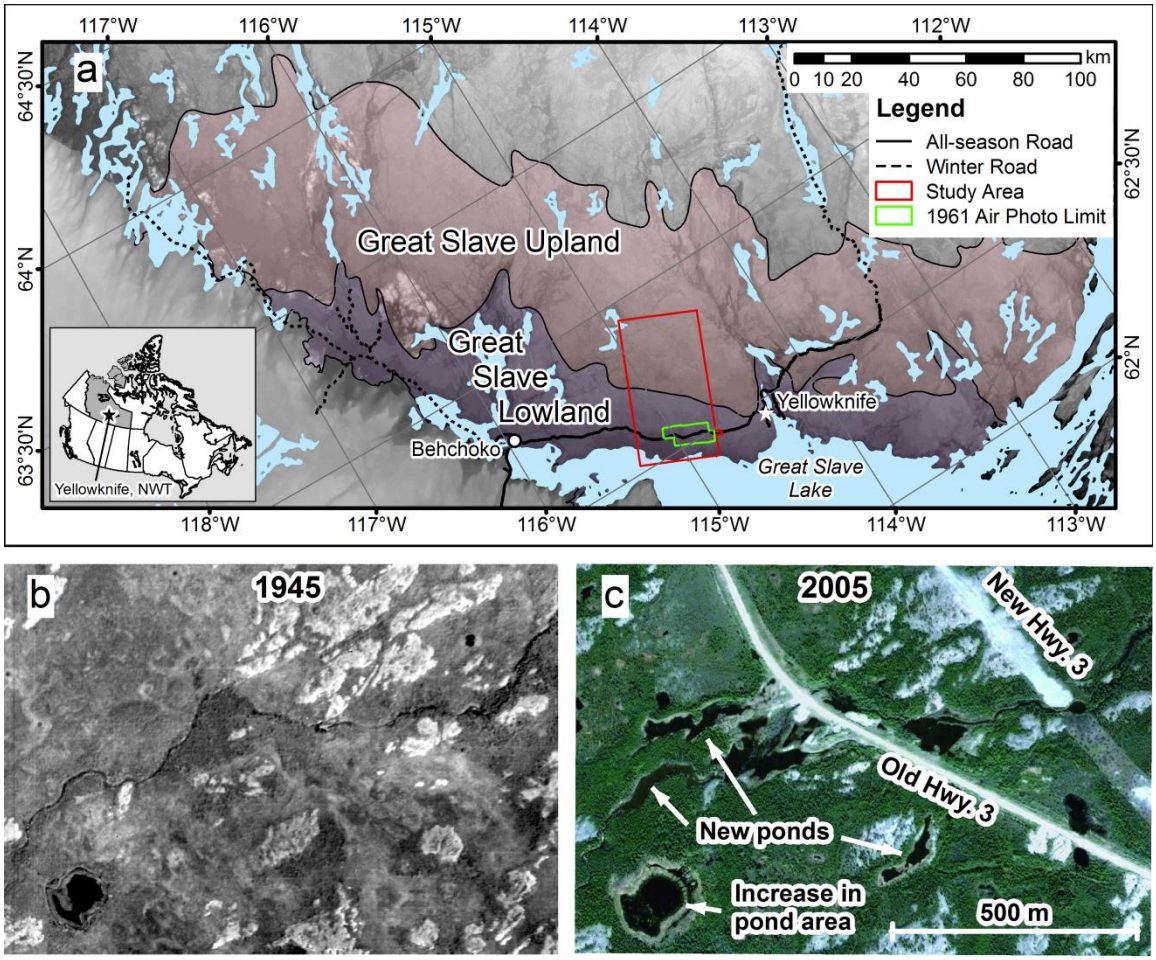

Figure 1. (a) Location of the study area (red polygon) with extent of 1961 air photos indicated (green polygon). (b) Representative subset of the study area near Northwest Territories Highway 3. (c) Thermokarst ponding development (a change from forest to water) and highway construction within the subset over a 60-year period; At some locations the water body is entirely new, and at others the water body has increased in size.

more extensive. Thus, the study area is generally oriented northeast to southwest along the regional topographic gradient. Further, because construction of the Highway 3 in the mid-1960s utilized locally-available fine-grained materials sourced along the right-of-way (Wolfe *et al.* 2011b), we examined potential thermokarst initiation at those sites and compared ponding adjacent to the highway with results for the region. The research objectives were to: (i) create a data capture methodology to enable change detection between images from 1945, 1961, and 2005; (ii) develop a work flow strategy to ensure quick, efficient, and thorough data capture; and (iii) utilize an approach that makes a distinction between natural and anthropogenic thermokarst.

2 BACKGROUND

Located in the southern portion of the Slave Geological Province of the Canadian Shield, the study area is bordered by the North Arm of Great Slave Lake to the south and by the Taiga Shield Low Subarctic ecoregion to the north (Ecosystem Classification Group 2008) (Figure 1a). Discontinuous permafrost up to 50 m thick occurs beneath a 0.30 to 1.30 m thick active layer (Brown 1973; Morse *et al.* 2015). Permafrost is present within fine-grained sediments overlain by peatlands and forests that may be black spruce (*Picea mariana*) dominated, mixed deciduous and coniferous forests, or pure stands of white birch (*Betula papyrifera*) (Morse *et al.* 2015), but not beneath bedrock outcrop or coarse grained unconsolidated sediments (Brown 1973). The mosaic of forests and peatlands is perforated by numerous waterbodies.

Discontinuous permafrost terrain in this region has a relatively recent history that is reflected by the two prominent ecoregions the Great Slave Lowland (GSL) and Great Slave Upland (GSU) (Ecosystem Classification Group 2008) (Figure 1a). Following retreat of the Laurentide Ice Sheet, glacial Lake McConnell established in the region between about 12 700 and 9 300 cal BP. As a consequence of inundation by glacial Lake McConnell and ancestral Great Slave Lake, the upland is characterized by thin discontinuous deposits of wave-washed tills, glaciolacustrine sediments and glaciofluvial materials occurring between bedrock outcrops. In contrast, the lowland features prominent glaciolacustrine deposits that cover nearly 70 % of the exposed surface (Wolfe at al. 2014b). Lake level recession over the last 8000 years occurred at a rate of about 5 $mm \cdot a^{-1}$ in the Yellowknife area, and permafrost aggraded into fine-grained sediments post-dating terrestrial emergence (Wolfe and Morse 2016). Throughout much of the region ground ice accumulation likely accompanied permafrost aggradation, as is evident by widespread lithalsa occurrence in the GSL and GSU (Wolfe at al. 2014b).

Climatic conditions control permafrost aggradation in exposed terrain. Climate normal data (1981–2010) from Yellowknife Airport (YZF) (Environment Canada 2016) indicate regional climate is subarctic continental, winters are cold (-25.6 °C January mean), summers are warm (17.0 °C July mean), mean annual air temperature (MAAT) is -4.1 °C, and of the 29 mm of annual precipitation, about 40 % is derived from snowfall

(Environment Canada 2016). Prior to 6000 cal BP regional climate was cooler than present and subaerial GSU was dominated by tundra, shrub tundra and taiga (Huang *et al.* 2004). Between 6000 and 3500 cal BP the climate warmed and treeline moved north (Moser and MacDonald 1990; MacDonald *et al.* 1993), but with subsequent cooling beginning around 3000 cal BP treeline moved south to its present position (Huang *et al.* 2004). Since the 1940s, Yellowknife annual mean air temperatures have increased (Riseborough *et al.* 2013), and since the 1971–2000 climate normal, MAAT has increased 0.5 °C, in accord with the pan-Arctic warming trend beginning AD 1966 (Intergovernmental Panel on Climate Change 2013).

Regional climate warming has resulted in disequilibrium permafrost thermal conditions demonstrated by: (1) inverted annual mean ground temperature profiles, (2) annual mean temperatures near the top of permafrost that are commonly greater than the annual mean temperatures at the depth of zero annual amplitude (DZAA; -1.4 °C to 0.0 °C), and (3) gradual increases in ground temperatures below DZAA (Morse *et al.* 2015; Wolfe *et al.* 2015). Relatively thin permafrost throughout the GSL exhibits signs of degradation (Figures 1b and 1c), and Zhang *et al.* (2014) predict that permafrost extent in this region will be reduced to 2.5% by 2090s, with permafrost limited to peatlands. The predicted reduction rates may be exaggerated without the inclusion of latent heat effects (Morse *et al.* 2015), but conversely, three-dimensional permafrost degradation that occurs in discontinuous permafrost conditions (*e.g.*, McClymont *et al.* 2013) is unaccounted for by Zhang et al (2014).

The heterogeneous terrain of GSL is traversed by a 105-km segment of Highway 3 that runs sub-parallel to the north shore of Great Slave Lake, from Behchoko to Yellowknife (Figure 1a). The highway alignment preferentially crossed terrain underlain by fine-grained sediments to avoid bedrock and waterbodies. Shallow borrow pits were developed in the mid-1960s along the right-of-way to source local silt and clay for highway embankment construction (Wolfe *et al.* 2011b). Following development, many borrow pits have ponded with water (Wolfe *et al.* 2011b). Between 1999 and 2006, major highway realignments maximized bedrock traverses to minimize the extent of thaw sensitive terrain crossed by the highway and thus embankment settlement (Wolfe *et al.* 2015). Realignment sections are constructed with open graded blast-rock (30 cm and less) embankments. Water is ponded along embankment sections where topographic depressions occur either naturally or due to subsidence (Stevens and Wolfe 2012) and where natural flow was interrupted.

3 STUDY AREA

Positioned approximately 20 km northeast of Yellowknife (Figure 1), the nearly1430 km^2 study area is generally oriented northeast to southwest along the regional topographic gradient in order to test the hypothesized relation between thermokarst and elevation. Surficial geology mapping based on Landsat 7 imagery from 2001 indicates the extent of

bedrock outcrop (R), glaciolacustrine (GL), glaciofluvial (GF), anthropogenic (H), and organic (O) deposits, and water bodies (W) within this study area (Stevens *et al.* 2012a), allowing us to test for a relation between thermokarst and surficial materials. The study area captures a ~30-km long segment of Highway 3 which enables us to test the hypothesis that thermokarst was been initiated by highway and borrow pit development.

4 METHODS

4.1 Data

The inventory of thermokarst was developed by digitizing the location of areas forested in the past as noted on historical air photos onto more recent satellite-based images where water is present. This was accomplished by comparing National Air Photo Library (NAPL) panchromatic air photos from 1945 and 1961 (Table 1) with colour QuickBird2™ images from 2005 by DigitalGlobe™ displayed in Google Earth™. Air photos (n=140) from 1945 (1:25000) were scanned at 800 dpi giving a 0.80 m pixel resolution, and photos (n= 19) from 1961 (1:17400) were scanned at 400 dpi giving a 1.1 m pixel resolution. QuickBird2 images were from 2005 and had a display resolution in Google Earth™ of about 0.60 cm.

4.2 Digitization

Digitized thermokarst pond polygons were sorted in to three categories according to time: 1945 – 2005; 1945 – 1961; 1961-2005. Polygons for "1945-2005" delineate water that ponded between the 1945 air photo and the 2005 satellite image. Those polygons within the sub-regional extent of 1961 air photos (Figure 1) for "1945 – 1961" delineate water that ponded between the 1945 and 1961 air photos, and those for "1961 – 2005" delineate water that ponded between the 1961 air photo and 2005 satellite image.

Digitization was carried out by displaying a scanned air photo on one half of a high resolution computer monitor, and displaying the 2005 satellite image in Google Earth™ on the other half. Image extents and scales of the air photo and satellite image were matched as closely as possible on the display, and ponding evident in the satellite image was manually digitized in Google Earth™ using the "Polygon" tool. The margin of error for an individual pond area is likely on the order of ±50 m^2. Digitized polygons were exported from Google Earth™ to ArcGIS™ for spatial analysis.

Ponding was characterized by a change from forest to water based on differences in spectral characteristics, texture, and shape. In the air photos, the pond is most often recognized by the dark and uniform tone associated with water. In some cases, due to sun angle during image capture, the pond could appear as a lighter gray than the surrounding terrain. If conditions were windy the pond could appear to have ripples. Where there was variability in the colour or surface characteristics of the pond, the overall shape of the pond, often round or oval, was a reliable indicator. Treed areas in the air photos often

Table 1. Flight lines and photo information for historical air photos used in the study.

Line	Year	Date	Altitude (feet)	Focal length (mm)	Scale	Photo numbers	Photo count (n)
A8561	1945	13-Jul	11600	153.49	1:25000	13, 15, 17, 19, 54, 56, 58, 60, 62, 64, 66, 68, 70	13
A8566	1945	13-Jul	11600	152.40	1:25000	9	1
A8662	1945	10-Jul	11600	153.49	1:25000	81, 83, 85, 87, 89, 91, 93, 95, 97	9
A8663	1945	22-Jul	11600	152.40	1:25000	22, 24, 26, 28, 30, 32, 34, 36, 38	9
A8664	1945	22-Jul	11600	152.40	1:25000	80, 82, 84, 86, 88, 90, 92, 94, 96	9
A8665	1945	22-Jul	11600	152.40	1:25000	24, 26, 28, 30, 32, 34, 36, 38, 40	9
A8666	1945	13-Jul	11600	152.40	1:25000	84, 86-92, 111, 113	10
A8667	1945	19-Jul	11600	152.40	1:25000	5, 3, 7, 9, 11, 13	6
A8668	1945	22-Jul	11600	152.40	1:25000	83-89, 108, 110, 112, 114, 116, 118, 120	14
A8669	1945	22-Jul	11600	152.40	1:25000	129, 131, 133, 135, 137, 139, 141, 143, 145	9
A8670	1945	22-Jul	11600	153.49	1:25000	80, 82, 84, 86, 88, 90, 92, 94, 96	9
A8671	1945	22-Jul	11600	153.49	1:25000	33, 35, 37, 39, 41, 43, 45, 47, 49	9
A8672	1945	22-Jul	11600	152.40	1:25000	63, 65, 67, 69, 71, 73, 75, 77, 79	9
A8743	1945	24-Jul	11600	152.40	1:25000	30, 32, 34, 36, 38, 40, 42	7
A8744	1945	24-Jul	11600	152.40	1:25000	32, 34, 36, 38, 40, 112, 114, 116	8
A8750	1945	24-Jul	11600	152.40	1:25000	29, 31, 33, 35, 37, 39, 41, 43, 45	9
A17494	1961	16-Sep	8700	152.14	1:17400	105-114	10
A17495	1961	16-Sep	8700	152.14	1:17400	35-43	9

have a texture related to the canopy and have a tone that is lighter than water, yet darker than other surrounding low vegetation due to shadows. Burned areas have little apparent texture and are lighter in tone than treed areas. Bedrock outcrops are very light and bright in comparison, have shaded areas indicative of relief, and have textures indicative of geological structures. The QuickBird2™ imagery has the added benefit of colour. Ponds once again are the most obvious features in the imagery, being dark, rounded, and smooth textured. Vegetated areas are slightly easier to discern as the canopy of varying species can be identified with shape and colour, areas of dying vegetation are seen as a grayish brown, and ground cover or short vegetation lacks shadow and therefore is lighter. Bedrock outcrops often appear in light to medium shades of gray.

Ponding between 1961 and 2005 was mapped first, then ponding between 1945 and 1961, and then ponding within the rest of the study area between 1945 and 2005. If a pond visible in the QuickBird2™ image was clearly a treed area in the air photo, the pond extent was digitized and labeled in Google Earth™. If an existent pond in the air photo expanded between image dates, or new ponding was found within a close proximity to an existent pond, then the new ponding was digitized and labeled.

4.3 **Analysis**

All digitized ponds were combined into one file with attributes indicating one of the three time periods for pond formation. To examine the influence of surficial geology, a point file of pond centroids was generated and used to assign the surficial geology value to each polygon. Recognizing the potential for the centroid to fall within a surficial geology polygon that is different from the surficial geology unit overlain by the majority of the pond polygon, there may be some error associated with the method, but this is likely minimal due to the generally homogeneous surficial geology at the scale of the mapped ponding. The centroids were also used to assign elevation values to the polygons.

Assessment of thermokarst ponding in the vicinity of the original Highway 3 was done by selecting digitized polygons that intersect a 200 m buffer created from the highway centreline and assigning this proximity to the polygon with a new attribute. In order to assess the relation of borrow pits to ponding, and attribute was assigned to all ponds that intersected a borrow pit (borrow pit data are from Wolfe *et al.* 2011b). Finally, all ponding within the 1961 sub-area were assigned an attribute as such in order to determine the relation between background thermokarst and the potential effects of Highway 3 development. Once all attributes were assigned to the polygons, analysis was carried out by querying the polygon attributes.

4.4 **Limitations**

The main objective of this research is a first order estimation of thermokarst ponding. As such, the digitizing process involved expert decision that, though dependent on personal interpretation, was deemed sufficient to fulfill the objectives at hand. It is recognized that

variation of water extent between years may relate to water level variation that can be affected by variable meteorological conditions. Therefore, we took a conservative approach and considered thermokarst ponding to have developed when the land cover changed from forest to water. Thus we did not map pond extent changes that might have simply been related to a change in meteorological conditions.

To demonstrate that thermokarst is active within this study area, we utilize only three image dates. This limits our ability to make inferences about rates of change over time, but it is adequate for the stated objectives.

As ponds are digitized on the Google Earth™ image base, some localized georeferencing problems may occur in relation to the position of the imagery shown, but these individual errors are not considered significant as the results are considered in aggregate.

5 RESULTS

5.1 Within the Study Area

Over a 60 year period (1945-2005), 3138 thermokarst ponds developed or expanded within the study area (Figures 2 and 3). Approximately 3.57 km^2 of land cover converted from forest to pond (~0.25 % of the study area), and most ponds are small (n = 3025) with an area of less than 5000 m^2 (Figure 3a).

From the total set, 2903 new ponding sites (~3.31 km^2) are located below 210 m a.s.l., with only 235 (~0.26 km^2) located above (Figures 2, 4b, and 5a), thus the majority of newly ponded area is located within GSL. Whereas the counts of new thermokarst ponding sites declines as elevation increases (Figure 5a), ponded size is largely independent of elevation (Figure 4b).

With respect to the surficial geology, nearly 76% of the ponds are located within glaciolacustrine deposits and about 20% are within terrain mapped as water. Remaining ponds are located within bedrock (4%), anthropogenic (< 1%), and organic (< 1%) deposits (Figures 3 and 5b).

5.2 Within the 1961 Sub-area

Within the 1961 sub-area (103.76 km^2) 552 instances of thermokarst ponding were mapped (Figure 6). Of the 447 ponds that are not within borrow pits, 158 formed between 1945 and 1961 (16 years) and 289 between 1961 and 2005 (44 years).

5.3 Influence of Highway 3

In the vicinity of the old alignment, 270 instances of thermokarst ponding in the study area intersect a 200-m buffer of the highway, 148 of which are within borrow pits and 122 are not. Within the 1961 sub-area (Figure 6) 171 pondings occur within 200 m of the highway alignment, but only 11 formed between 1945 and 1961. Of the remaining 160 pondings that formed between 1961 and 2005, 104 are located within borrow pits. There

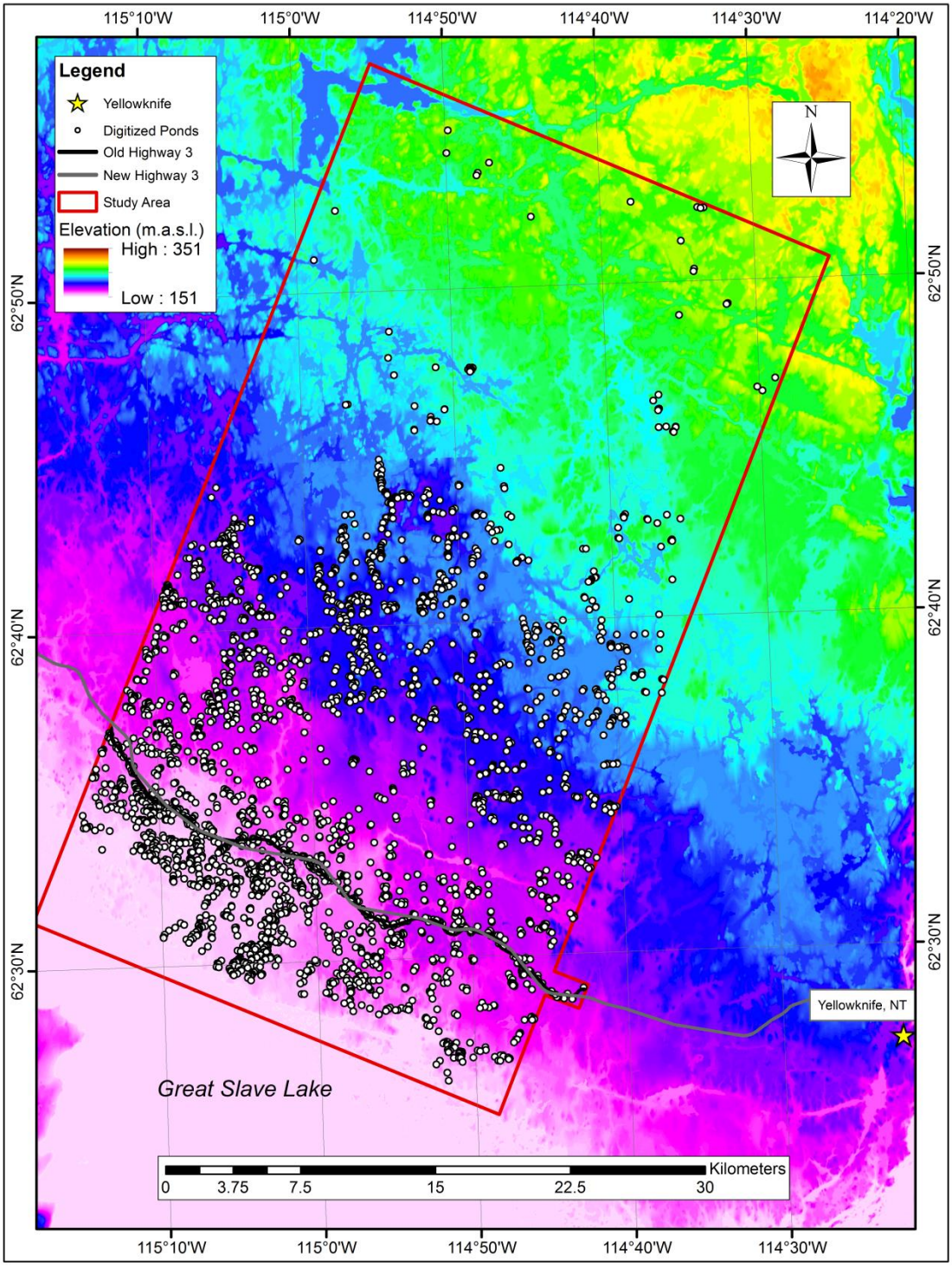

Figure 2. Location of mapped thermokarst ponding in relation to elevation in the North Slave region.

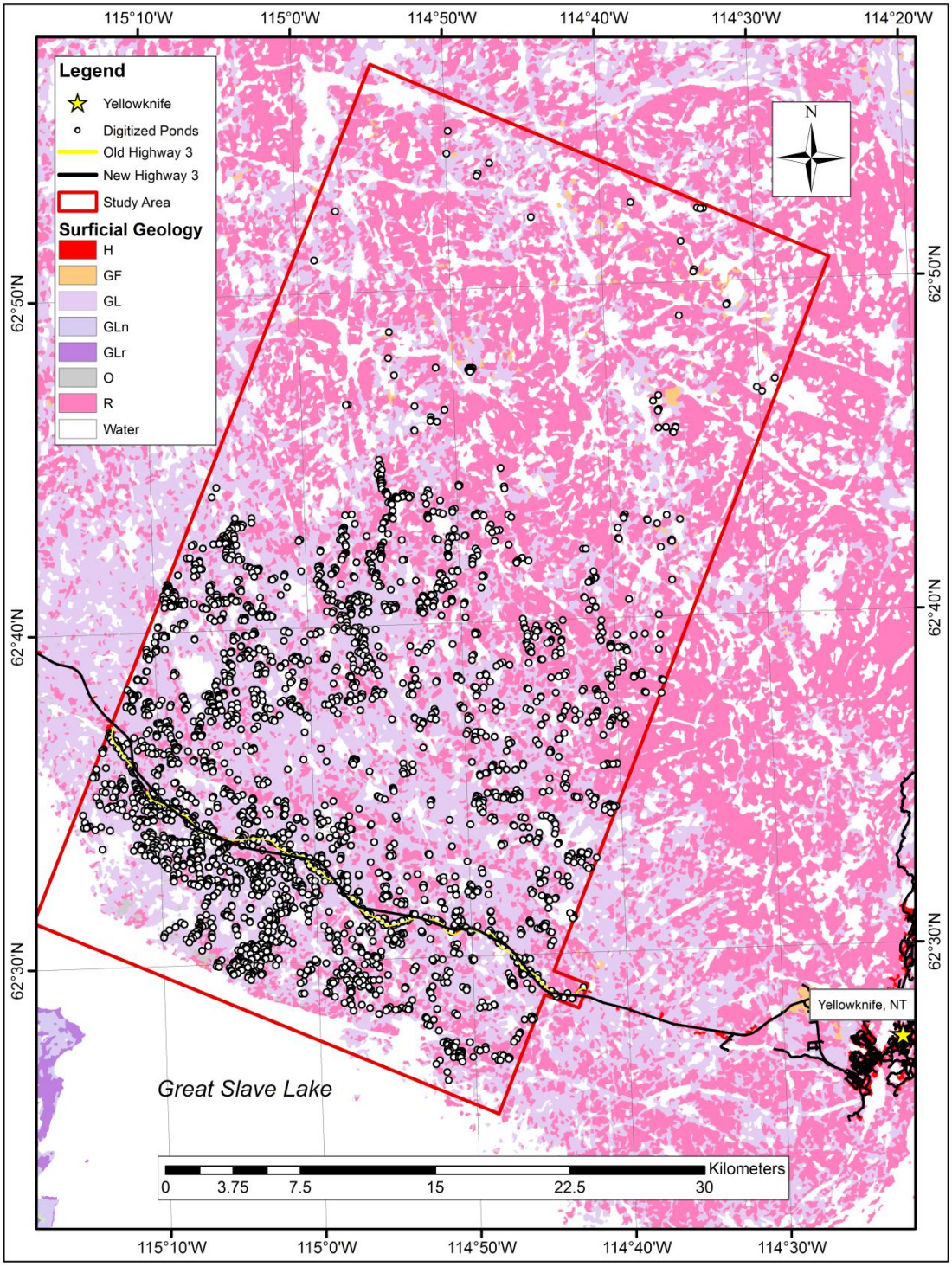

Figure 3. Location of mapped thermokarst ponding in relation to surficial geology in the North Slave Region. Surficial geology data are from Stevens *et al.* 2012.

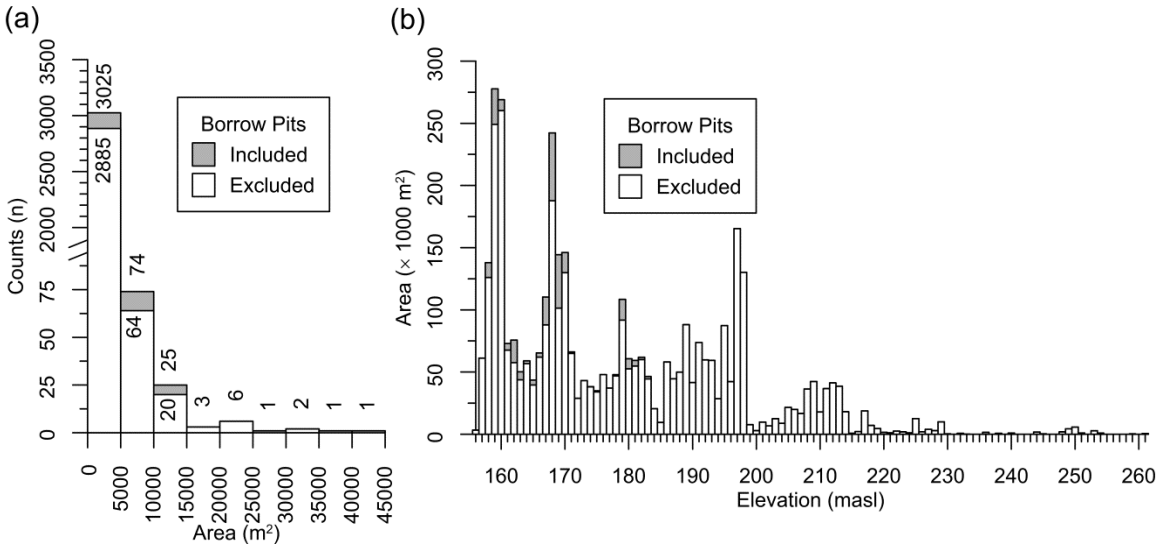

Figure 4. (a) Frequency distribution of thermokarst ponded areas for full study area (1945 to 2005) including (total area = 3 572 511 m^2) and excluding (total area = 3 311 412 m^2) ponded areas associated with borrow pits (borrow pit pond area = 261 098 m^2). (b) Relation between elevation and thermokarst pond area for full study area (1945 to 2005) including and excluding borrow pit ponds.

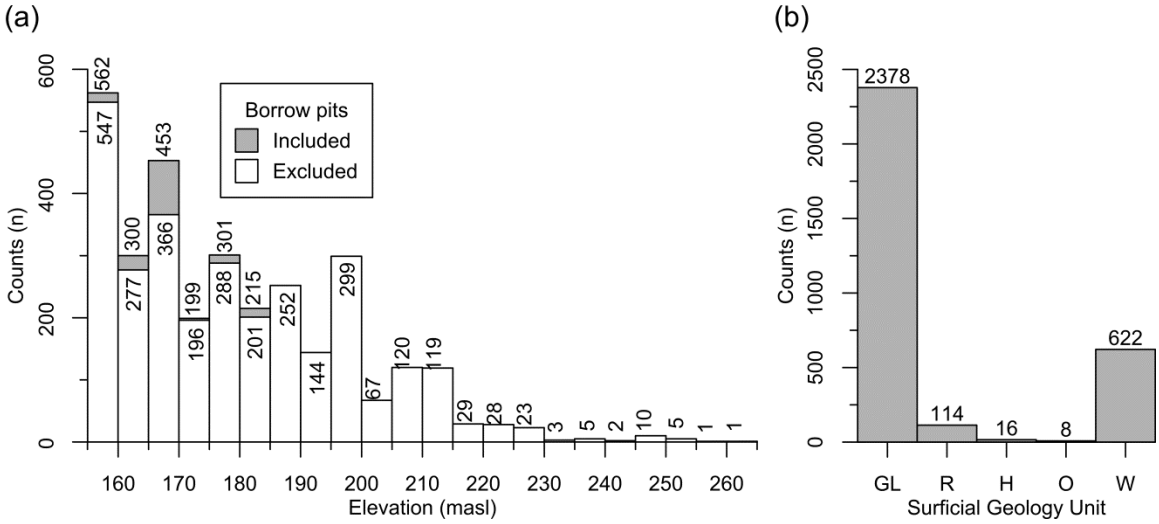

Figure 5. Frequency distributions of thermokarst ponding within the full study area (1945 to 2005) with respect to: (a) elevation including (n = 3138) and excluding (n = 2983) the 155 ponded areas associated with borrow pits; (b) surficial geology (GL = glaciolacustrine; R = rock; H = anthropogenic; O = organic; W = water).

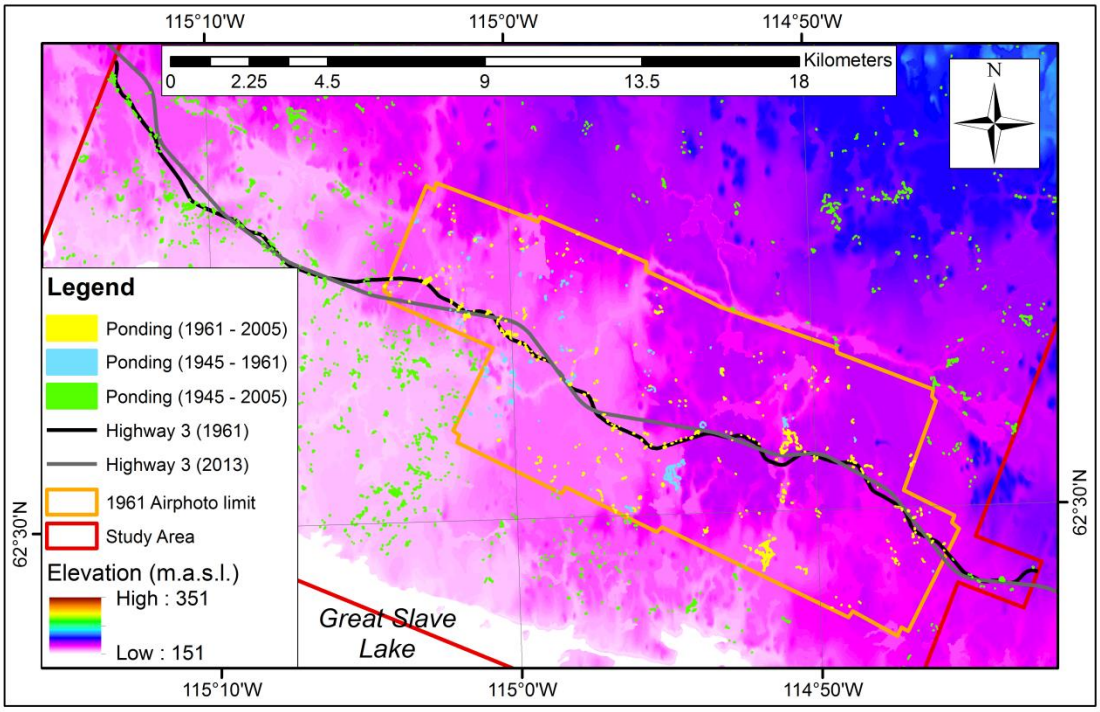

Figure 6. Thermokarst ponding mapped in the vicinity of Northwest Territories Highway 3, with the 1961 air photo limit indicated.

are 164 borrow pits excavated along old highway within the study area and 87 of them intersect ponded areas (n = 155). Of the 112 borrow pits within the 1961 sub-area, 56 borrow pits intersect with 105 pondings, only 1 of which began development between 1945 and 1961. Noticeably, not every borrow pit features a ponded area, and several borrow pits have more than one ponded area.

6 DISCUSSION

Thermokarst development (a change from forest cover to water) over 60 years (1945 to 2005) is widespread in the study area and likely throughout the region. Within the study area, thermokarst ponding (~3.57 km^2) is equivalent to about 0.08% of the land area (4348.8 km^2). The relatively small overall proportion of ponding is likely because the individual area of most (96%) of the 3138 thermokarst ponds that developed between 1945 and 2005 is less than 5000 m^2.

The location of thermokarst ponding is related to the distribution of fine-grained deposits associated with ground ice distribution in this region. With respect to surficial geology, 96% of ponds (and 97% of total pond area) are associated with glaciolacustrine deposits, or water adjacent to glaciolacustrine deposits. As the surficial geology data are derived from recent (2001) satellite images by which time much of the thermokarst had occurred, many ponds with water as an attribute likely developed within glaciolacustrine deposits. Associations of ponds with water may also be related to a scaling effect of the low resolution Landsat 7 images (30-m pixels) from which the surficial geology is derived. Also, the position of the pond centroid used to extract surficial geology unit within the GIS, may fall within a water polygon, thought the majority of the pond may overlie a glaciolacustrine deposit polygon.

The distribution of thermokarst is related to elevation. More extensive thermokarst at lower elevations is likely due to more extensive deposits of fine-grained materials (Figure 3). Notably, a distinct reduction in ponded area and counts (Figures 4b and 5a) occur at about 215 m a.s.l., the upper elevation limit in this region for extensive sediments.

Most thermokarst ponding is primarily within GSL, largely as a function of the extent of low-elevation, fine-grained surficial materials. However, within GSL there is a relatively high density of thermokarst ponding in the vicinity of Old Highway 3 (Figure 6). Nearly 9% of all ponds are located within 200 m of the original highway alignment. In comparison to the pond area density of 0.08% within the land area of the entire study area, or 0.14% (glaciolacustrine deposits and water) of the land area within glaciolacustrine deposits, pond area density within the 200 m highway buffer area is 2.5%. As observed within the 1961 sub-area, a majority (~71%) of ponds formed between 1961 and 2005. However, ~94% of the 171 ponds within 200 m of the original highway centerline developed over the same time period, and ~61% developed in borrow

pits. About half of all borrow pits in the study area, and within the sub-area, intersect thermokarst ponds.

7 SUMMARY AND CONCLUSIONS

This Open File provides an inventory of thermokarst ponding that developed between 1945 and 2005 in a study area that is representative of the region. Thermokarst ponded area are generally small (< 5000 m^2), but range up to nearly 45 000 m^2. The distribution of thermokarst ponding is closely related to elevation and surficial geology, with ponding dominantly constrained to glaciolacustrine deposits, and decreased ponding counts with increased elevation. Consequently, thermokarst development is most common within GSL, and is rare within GSU. In comparison with ponding density within glaciolacustrine deposits, ponding density is an order of magnitude greater in the vicinity of the original Highway 3 that crosses GSL. Within the study area, about half of the borrow pits established for highway construction have developed thermokarst ponding within them. Nearly all ponding within 200 m of the highway has been since 1961, though thermokarst pond development in the region has been ongoing since at least the mid-1940s.

Thermokarst is widespread throughout the region with numerous thermokarst ponds as GL deposits are extensive. Reduced thermokarst ponding at higher elevation is likely related to reduced GL extent, but may also be related to more time for past thermokarst development given the landscape history. Regardless, future thermokarst development will continue to be associated with permafrost in low lying forested GL deposits that should be avoided by new infrastructure construction.

ACKNOWLEDGMENTS

Digitization of thermokarst ponds by Taylor McWade was undertaken during her placement at the GSC through a practicum program administered by the Department of Geography and Environmental Studies, Carleton University.

REFERENCES

BGC Engineering Inc. 2011. *Highway 3 – Climate Change Vulnerability Assessment. Report*, August 10, 2011.

Brown RJE. 1973. Influence of climatic and terrain factors on ground temperatures at three locations in the permafrost region of Canada. In *Proceedings of the Second International Conference on Permafrost, North American Contribution*, 13–28 July 1973, Yakutsk, USSR. National Academy of Sciences: Washington, DC, USA; 27–34.

Ecosystem Classification Group. 2008. *Ecological Regions for the Northwest Territories – Taiga Shield*. Government of the Northwest Territories: Yellowknife, NT, Canada; 149 pp.

Environment Canada. 2016. Climate Data Online. http://climate.weather.gc.ca/ [13 November 2016].

French HM. 2007. *The Periglacial Environment*, 3rd edition. Longman: London, UK. 458 pp.

Heginbottom JA, Dubreuil MA, Harker PA. 1995. Canada-Permafrost. In *National Atlas of Canada*, Fifth Edition. National Atlas Information Service, Natural Resources Canada: Ottawa, ON, Canada; Plate 2.1. MCR 4177.

Huang C, MacDonald GM, Cwynar LC. 2004. Holocene landscape development and climate change in the Low Arctic, Northwest Territories, Canada. *Palaeogeography Palaeoclimatology Palaeoecology* **205**: 221–234. DOI:10.1016/j.palaeo.2003.12.009

Intergovernmental Panel on Climate Change. 2013. *Climate Change 2013: The Physical Science Basis. Contribution of Working Group I to the Fifth Assessment Report of the Intergovernmental Panel on Climate Change*, Stocker TF, Qin D, Plattner G-K, Tignor M, Allen SK, Boschung J, Nauels A, Xia Y, Bex V, Midgley PM (eds). Cambridge University Press: Cambridge, UK and New York, NY, USA; 1535 pp.

MacDonald GM, Edwards TWD, Moser KA, Pienitz R, Smol JP. 1993. Rapid response of treeline vegetation and lakes to past climate warming. *Nature* **361**: 243–246. DOI:10.1038/361243a0

McClymont FA, Masaki H, Bentley LR, Christensen BS. 2013. Geophysical imaging and thermal modeling of subsurface morphology and thaw evolution of discontinuous permafrost. *Journal of Geophysical Research, Earth Surface* **118**: 1826–1837. DOI:10.1002/jgrf.20114.

Morse PD, Wolfe SA, Kokelj SV, Gaanderse AJR. 2015. The Occurrence and Thermal Disequilibrium State of Permafrost in Forest Ecotopes of the Great Slave Region, Northwest Territories, Canada. *Permafrost and Periglacial Proces*ses **27**: 145-162. doi:10.1002/ppp.1858

Moser KA, MacDonald GM. 1990. Holocene vegetation change at treeline Northwest Territories, Canada. *Quaternary Research* **34**: 227–239. DOI:10.1016/0033-5894(90)90033-h

Olthof I., Fraser RH, Schmitt C. 2015. Landsat-based mapping of thermokarst lake dynamics on the Tuktoyaktuk Coastal Plain, Northwest Territories, Canada since 1985. *Remote Sensing of the Environment* **168**: 194-204. doi:10.1016/j.rse.2015.07.001

Seto JTC, Arenson LU, Cousineau G. 2012. Vulnerability to climate change assessment for a highway constructed on permafrost. *In Proceedings, Cold Regions Engineering 2012: Sustainable Infrastructure Development in a Changing Cold Environment*, 19-22 August 2012, Québec City, Canada, Morse, B. and Doré G. (eds.). American Society of Civil Engineers: 515-524. doi:10.1061/9780784412473.051

Stevens CW, Wolfe SA. 2012. High-resolution mapping of wet terrain within discontinuous permafrost using LiDAR intensity. *Permafrost and Periglacial Processes* **23**: 334-341. doi:10.1002/ppp.1752

Stevens CS, Kerr DE, Wolfe SA, Eagles S. 2012a. Predictive surficial materials and geology derived from LANDSAT 7, Yellowknife, NTS 85 J, Northwest Territories. *Geological Survey of Canada, Open File 7108*. Geological Survey of Canada: Ottawa, ON, Canada; 31 pp. doi:10.4095/291731

Stevens CW, Short N, Wolfe SA. 2012b. Seasonal surface displacement and highway embankment grade derived from InSAR and LiDAR, Highway 3 west of

Yellowknife, Northwest Territories. *Geological Survey of Canada, Open File 7087*. Geological Survey of Canada: Ottawa, ON, Canada; 112 pp. doi:10.4095/291383

Wolfe SA, Morse PD. 2016. Lithalsa formation and holocene lake-level recession, Great Slave Lowland, Northwest Territories. *Permafrost and Periglacial Proces*ses. **27.** Published online in Wiley Online Library (wileonlinelibrary.com). doi:10.1002/ppp.1901

Wolfe SA, Duchesne C, Gaanderse A, Houben AJ, D'Onofrio RE, Kokelj SV, Stevens CW. 2011a. Report on 2010–2011 Permafrost investigations in the Yellowknife area, Northwest Territories. *Geological Survey of Canada, Open File 6983, Northwest Territories Geoscience Office, NWT Open Report 2011-009*. Geological Survey of Canada: Ottawa, ON, Canada; 75 pp. doi:10.4095/289596

Wolfe SA, Delaney S, Duchesne C. 2011b. An inventory of borrow pits and pond development between 1961 to 2005, Highway 3, Yellowknife Region, Northwest Territories. *Geological Survey of Canada, Open File 6948*. Geological Survey of Canada: Ottawa, ON, Canada; 42 pp. DOI:10.4095/289032

Wolfe SA, Short NH, Morse PD, Schwarz SH, Stevens CW. 2014a. Evaluation of RADARSAT-2 DInSAR seasonal surface displacement in discontinuous permafrost terrain, Yellowknife, Northwest Territories, Canada. *Canadian Journal of Remote Sensing* **40**:406–422. doi:0.1080/07038992.2014.1012836

Wolfe SA, Stevens CW, Gaanderse AJ, Oldenborger GA. 2014b. Lithalsa distribution, morphology and landscape associations in the Great Slave Lowland, Northwest Territories, Canada. *Geomorphology* **204**: 302-313. doi:10.1016/j.geomorph.2013.08.014

Wolfe SA, Morse PD, Hoeve TE, Sladen WE, Kokelj SV, Arenson LU. 2015. Disequilibrium permafrost conditions on NWT Highway 3. Paper 115 in *Proceedings, 68rd Canadian Geotechnical Conference and 7th Canadian Permafrost Conference*, Quebec City, Quebec. Canadian Geotechnical Society, Richmond, British Columbia, 8 pp.

Zhang Y, Olthof I, Fraser R., Wolfe SA. 2014. A new approach to mapping permafrost and change incorporating uncertainties in ground conditions and climate projections. *The Cryosphere* **8**: 2177-2194. doi:10.5194/tc-8-2177-2014

Zhang Y, Wolfe SA, Morse PD, Olthof I, Fraser RH. 2015. Spatiotemporal impacts of wildfire and climate warming on permafrost across a subarctic region, Canada. *Journal of Geophysical Research: Earth Surface* **120**: 2338-2356. doi:10.1002/2015JF003679

APPENDIX A - FGDC COMPLIANT METADATA

<metadata>

<idinfo>

<citation>

<citeinfo>

<title>TKP_UTM11NAD83</title>

<geoform>vector digital data</geoform>

</citeinfo>

</citation>

<descript>

<abstract>This open file provides an inventory of thermokarst pond development between 1945 and 2005 in a study area that is representative of the southern North Slave region between Behchoko and Yellowknife, Northwest Territories. The primary purpose of this inventory is to approximate the location and size of thermokarst ponds in a study area representative of the region to assist in better understanding present and future permafrost conditions. Because construction of the GNWT Highway 3 in the mid-1960s utilized locally-available fine-grained materials sourced along the right-of-way, we examine potential thermokarst initiation at those sites and compare ponding adjacent to the highway with results for the region. The inventory and database were prepared to evaluate the dominant controls on the distribution of thermokarst in the region, and the potential influence that highway construction may have had on thermokarst development. The accompanying shapefile format data can be used in a GIS to place areas of thermokarst ponds onto digital maps for referencing.</abstract>

<purpose>These data provide an inventory of thermokarst ponding that developed between 1945 and 2005 in a study area that is representative of the region. </purpose>

</descript>

<spdom>

<bounding>

<westbc>-115.258026</westbc>

```
      <eastbc>-114.471451</eastbc>
      <northbc>62.918938</northbc>
      <southbc>62.433142</southbc>
    </bounding>
  </spdom>
  <keywords>
    <theme>
      <themekt>None</themekt>
      <themekey>Thermokarst</themekey>
      <themekey>North Slave</themekey>
      <themekey>Great Slave Lowland</themekey>
      <themekey>Highway 3</themekey>
    </theme>
  </keywords>
  <accconst>None</accconst>
  <useconst>None</useconst>
  <datacred>Morse, P.D., McWade, T.L., Wolfe, S.A., 2017. Thermokarst ponding, North Slave region, Northwest Territories; Geological Survey of Canada, Open File 8205, 1 .zip file. doi:10.4095/300531</datacred>
  <native>Microsoft Windows 7 Version 6.1 (Build 7601) Service Pack 1; Esri ArcGIS 10.1.1.3143</native>
 </idinfo>
 <spdoinfo>
  <direct>Vector</direct>
  <ptvctinf>
    <sdtsterm>
```

```
      <sdtstype>GT-polygon composed of chains</sdtstype>
      <ptvctcnt>3138</ptvctcnt>
    </sdtsterm>
  </ptvctinf>
</spdoinfo>
<spref>
  <horizsys>
    <planar>
      <mapproj>
        <mapprojn>NAD 1983 UTM Zone 11N</mapprojn>
        <transmer>
          <sfctrmer>0.9996</sfctrmer>
          <longcm>-117.0</longcm>
          <latprjo>0.0</latprjo>
          <feast>500000.0</feast>
          <fnorth>0.0</fnorth>
        </transmer>
      </mapproj>
      <planci>
        <plance>coordinate pair</plance>
        <coordrep>
          <absres>0.00000000222002416450095 6</absres>
          <ordres>0.00000000222002416450095 6</ordres>
        </coordrep>
        <plandu>meter</plandu>
```

```
      </planci>
    </planar>
    <geodetic>
      <horizdn>D North American 1983</horizdn>
      <ellips>GRS 1980</ellips>
      <semiaxis>6378137.0</semiaxis>
      <denflat>298.257222101</denflat>
    </geodetic>
  </horizsys>
 </spref>
 <eainfo>
  <detailed>
   <enttyp>
    <enttypl>TKP_UTM11NAD83</enttypl>
   </enttyp>
   <attr>
    <attrlabl>FID</attrlabl>
    <attrdef>Internal feature number.</attrdef>
    <attrdefs>Esri</attrdefs>
    <attrdomv>
     <udom>Sequential unique whole numbers that are automatically
generated.</udom>
    </attrdomv>
   </attr>
   <attr>
```

<attrlabl>Shape</attrlabl>
<attrdef>Feature geometry.</attrdef>
<attrdefs>Esri</attrdefs>
<attrdomv>
<udom>Coordinates defining the features.</udom>
</attrdomv>
</attr>
<attr>
<attrlabl>OID_</attrlabl>
</attr>
<attr>
<attrlabl>Name</attrlabl>
</attr>
<attr>
<attrlabl>Shape_Leng</attrlabl>
</attr>
<attr>
<attrlabl>Shape_Area</attrlabl>
<attrdef>Area of feature in internal units squared.</attrdef>
<attrdefs>Esri</attrdefs>
<attrdomv>
<udom>Positive real numbers that are automatically generated.</udom>
</attrdomv>
</attr>
<attr>

<attrlabl>XCentroid</attrlabl>
</attr>
<attr>
<attrlabl>YCentroid</attrlabl>
</attr>
<attr>
<attrlabl>19451961</attrlabl>
</attr>
<attr>
<attrlabl>BorPit</attrlabl>
</attr>
<attr>
<attrlabl>SG</attrlabl>
</attr>
<attr>
<attrlabl>Elev</attrlabl>
</attr>
<attr>
<attrlabl>19452005</attrlabl>
</attr>
<attr>
<attrlabl>19612005</attrlabl>
</attr>
<attr>
<attrlabl>200m</attrlabl>

```
      </attr>
      <attr>
        <attrlabl>1961Area</attrlabl>
      </attr>
    </detailed>
  </eainfo>
  <metainfo>
    <metd>20170412</metd>
    <metstdn>FGDC Content Standard for Digital Geospatial Metadata</metstdn>
    <metstdv>FGDC-STD-001-1998</metstdv>
    <mettc>local time</mettc>
  </metainfo>
</metadata>
```